IRRADIATION TEST UNDER ADVANCED PWR CONDITIONS IN THE HALDEN REACTOR AND POST-IRRADIATION EXAMINATION OF FUEL ROD CLADDINGS FROM DIFFERENT ZIRCONIUM ALLOYS

V.A. MARKELOV, V.V. NOVIKOV, N.S. SABUROV, A.YU. GUSEV, V.F. KON'KOV, M.M. PEREGUD
JSC "High-Technology Scientific Research Institute for Inorganic Materials" (JSC VNIINM), Moscow
A.B. DOLGOV
JSC "TVEL" Moscow
B.YU. VOLKOV, V. ANDERSSON
Institute for Energy Technology (IFE) Norway

ABSTRACT

According to the bilateral project between IFE (Halden, Norway) and JSC “TVEL”/ JSC “VNIINM”, the IFA-728 test assembly with fuel rods made of claddings from Russian alloys (E110opt, E110M, E125 and E635M) was irradiated in the Halden reactor to a maximum fuel burn-up of 53.3 MWd/kgU. Results of non-destructive interim inspections during irradiation and destructive post irradiation examinations (PIE) to study a resistance to corrosion and to creep as well as hydrogenation of the different alloys under advanced PWR conditions are presented. These results have been compared to the data obtained in autoclave oxidation tests for unirradiated samples. The best combination of the corrosion resistance and mechanical stability under irradiation at high lithium water chemistry (advanced PWR) in a Halden reactor PWR loop were shown by E110opt and E110M claddings alloys. However, the E110M cladding showed a lower irradiation creep strain than E110opt cladding provided similar corrosion resistance.

Keywords: cladding, alloy, corrosion, hydrogenation, creep strain, irradiation, Halden reactor

1. Introduction

Zr-Nb and Zr-Nb-Sn-Fe type alloys are used as fuel cladding materials in VVER and PWR reactors. The E110 [1] and E635 [2] alloys are used for VVER reactors and M5 [3] and ZIRLO [4] alloys are used in PWR reactors. Other alloys of the mentioned above systems are being developed and tested in research and commercial reactors [5-8]. One of the main goals of this type development is to enhance corrosion and creep strain resistance of the zirconium fuel rod claddings.

The Halden Reactor (Norway) LWR loops [9,10], in which water chemistry regimes (WCR) and irradiation conditions are simulating PWR reactors, have been widely used in international practice for evaluating of corrosion characteristics of the developing alloys.

This paper presents the results of the bilateral project performed in the Halden reactor where the fuel test assembly IFA-728 with experimental fuel claddings from Russian alloys (E110opt, E110M, E125 and E635M) has been tested under high Li PWR water chemistry regime for direct comparison of the corrosion resistance, hydrogenation and irradiation creep. In addition, some results from irradiation of similar cladding samples from these alloys in the BOR-60 reactor on diametric creep under internal pressure also presented in the paper.

2. Materials, test conditions and research methods

Experimental fuel rod claddings with the outer diameter of 9.5 mm and the wall thickness of 0.57 mm manufactured from E110opt, E110M, E125 and E635M alloys, which compositions

are presented in the Table 1, have been used for the test. The tests claddings have a fully recrystallized structural state with the average grain size ~ 3 μm.
The experimental fuel rods with fuel column length of 200 mm were tested in the Halden reactor PWR loop at the temperature evaluated for the outer cladding surface on the level of 351 ºC in boron and high lithium (up to 10 ppm Li) WCR and with 2.0 % outlet void maintained during 907 effective days. Figure 1 shows schematically an axial elevation of the four fuel rods in the upper cluster UCl(5-8) and four fuel rods in the lower cluster LCl(1-4) in IFA-728 together with coolant temperature and burn-up distributions evaluated along the fuel assembly. One of the fuel rods from each alloy was loaded both in upper and lower cluster. The maximum burn-up level of 53.3 MW·day/kgUO_2 was accumulated in the low cluster fuel rods with claddings from E110opt and E110M alloys (Fig. 1).

Alloy	Nb, %	Sn, %	Fe, %	O, %
E110opt	1.05	-	0.055	0.085
E110M	1.02	-	0.095	0.120
E125	2.45	-	0.035	0.069
E635M	0.79	0.81	0.335	0.075

Tab 1: Alloying composition of the test fuel rod claddings

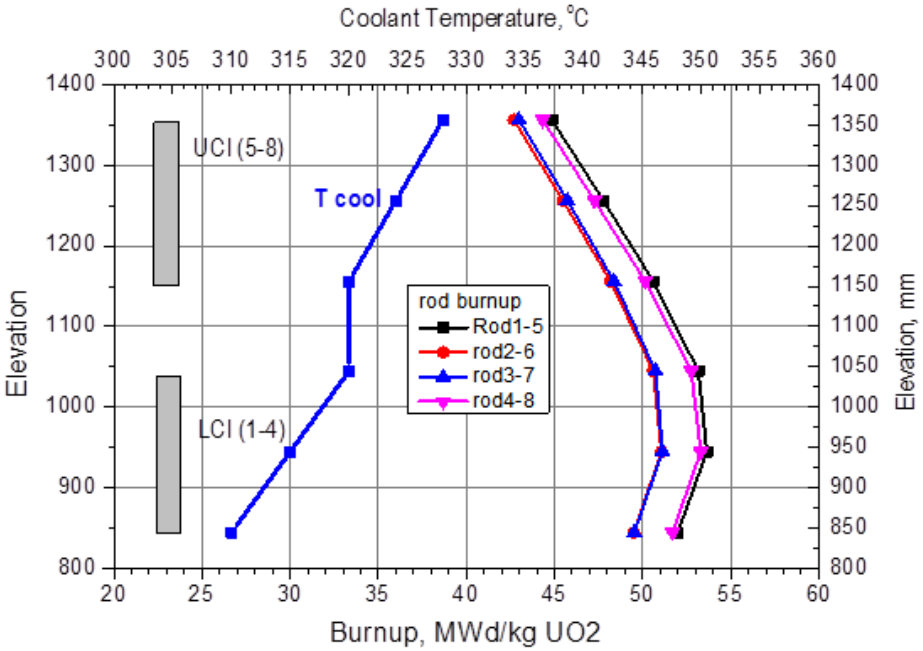

Fig. 1 – Coolant temperature and burn-up distributions along the height of IFA-728 with fuel rods in upper (UCl) and lower (LCl) clusters from the E110M (1 and 5), E125 (2 and 6), E635 (3 and 7) and E110opt (4 and 8) alloys

During irradiation monitoring of the cladding elongation in the lower cluster rods by means of in-pile detectors was performed as well as intermediate eddy-current oxide film thickness measurements in four sections of experimental fuel rod claddings placed in the upper cluster was performed.
After finishing irradiation, the inspection and destructive tests of the IFA-728 assembly were carried out including:
- visual assessment and photographing of the equipped samples of claddings located in the upper and lower clusters of the assembly;
- eddy-current measurement of the oxide layer thickness in four sections of the equipped claddings in the upper and lower clusters;
- diameter tracing measurement conducted along the fuel rods using three-pronged inductive sensor;

- elongation measurement by the distance between the pre-marked indicators on the fuel rod lower and upper plugs;
- metallographic analysis of structure and the oxide film thickness, distribution and orientation of hydrides;
- determination of hydrogen content by high-temperature extraction method.

In addition, a set of the fresh samples made from the same types of the cladding materials was tested in VNIINM in the autoclave at similar to IFA-728 water chemistry and cladding temperatures. Duration of the autoclave test was 930 days. The obtained results were compared to the Halden test IFA-728 to study effects of the irradiation on the corrosion and its acceleration.

3. Results on corrosion and hydrogenation resistance

Figure 2 shows the results of eddy-current measurements of the oxide film thickness during irradiation compared to the oxide film thickness after the autoclave tests. The data scatter bars characterize the minimum and maximum oxide film thickness achieved along the irradiated fuel rod claddings.

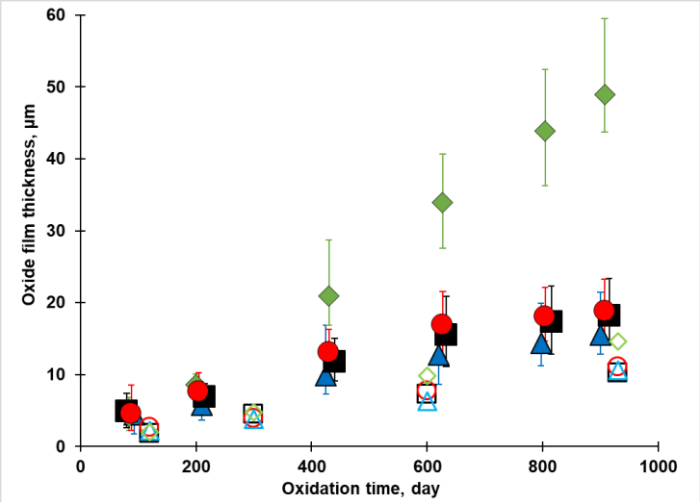

Fig.2 – Kinetics of the oxide film thickness growth of the test fuel rods (colored markers) compared to the data derived from the autoclave tests (uncolored markers): E110opt (■,□), E110M (●,○), E125 (▲, △), E635M (◆,◇)

The in-pile data showed that after 430 effective days of irradiation (burnup of 22.9 MW·day/kgUO_2) corrosion acceleration occurs in the E635M alloy cladding in contrast to autoclave tests. The oxide film thickness of the fuel rod cladding from the E635M alloy was 60 μm by the end of the test. The corrosion kinetics of the claddings from the E110opt, E110M and E125 alloys at this level of the fuel burn-up had tendency to slow down. The tests claddings made of the E125 alloy showed the best corrosion resistance. Claddings from the E110opt and E110M alloys have similar corrosion resistance both under autoclave and in-reactor conditions. A comparison of the in-reactor data and autoclave test results showed that oxide films thicknesses of all the investigated alloys under irradiation are higher than those observed under autoclave conditions (Fig. 2). Such difference in oxidation kinetics may be explained by heat rating from fuel in the cladding under in-reactor condition and higher temperature on a metal-oxide boundary in comparison with the estimated outer surface cladding temperature. The thicker the oxide film, the higher the temperature at the oxide-metal boundary. For the samples tested in the autoclave such effect is absent and cladding testing temperature is constant. According to metallography analysis the irradiation conditions increased the oxide film thickness formation on the surface of the cladding made of the E635M alloy (by 3.3 times) and have slightly influenced on the oxide thickness development on the E125 alloy cladding (by 1.3 times). Such values for E110opt and E110M alloys were about 1.8 and 1.6, respectively (see Table 2).

Based on the visual inspection of the fuel claddings from the E110opt, E110M and E125 alloys no sign of the oxide peeling has been observed and the claddings were covered by a dark oxide film. Oxide peeling was observed in some surface sections of the claddings made from the E635M alloy.

Alloy	Average oxide thickness (h), μm		h_R/h_A	Number of layers in oxide		Average layer thickness in oxide, μm	
	Autoclave	Reactor		Autoclave	Reactor	Autoclave	Reactor
E110opt	10.2	18.3	1.8	5	6	2.2	3.0
E110M	11.1	18.2	1.6	5	6	2.2	2.9
E125	10.6	13.6	1.3	4	4	2.6	3.2
E635M	14.7	48.8	3.3	7	-*	2.0	-*
h_R/h_A –oxide thickness ratio in reactor and in autoclave; * - it was impossible to determine							

Tab. 2: Metallography measurement results of oxide films after autoclave and reactor tests

Metallographic analysis of the oxide film morphology performed by optical (Figure 3b) and scanning electron (Figure 3a) microscopes allowed the data on non-destructive studies of the oxide film quality to be confirmed as well as to establish quantify the number of sub-layers in the films and their thickness. The morphology of the films depends on alloy composition and test conditions. Irradiation leads to increasing of sub-layers quantity (except the E125 alloy) and their thickness (Table 2).

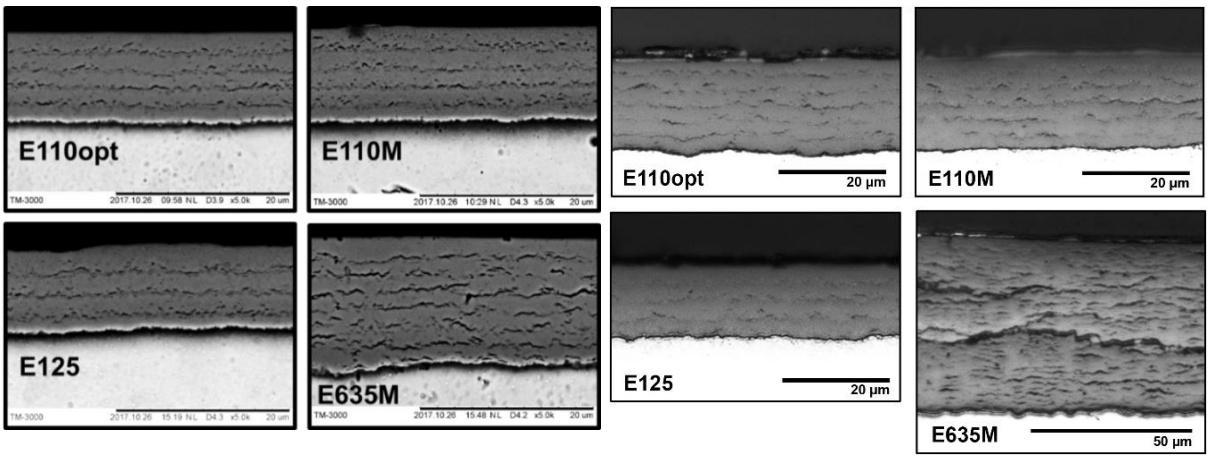

a b

Fig. 3 – Oxide films morphology of the investigated alloys after autoclave (a) and in-reactor (b) tests

Measurements of hydrogen content, which increases with increasing oxide layer thickness, were carried out in the process of the autoclave tests along with measurements of oxide films. It's noted that the oxide film of the E635M alloy is more prone to hydrogen permeation, because the hydrogen concentration in this alloy is higher compared to other alloys with similar oxide film thickness (Fig. 4). Hydrogen concentration determined in the samples tested in the autoclave is much higher than in the fuel rod claddings after irradiation in the Halden reactor. Such effect is explained by the fact that samples in autoclave test were oxidized both in outer and inner surfaces. The open ends of the sample in autoclave tests also insert certain contribution in the hydrogenation. In addition, water chemistry regime in the Halden reactor PWR loop was kept stable as opposed to the autoclave test.

According to metallographic analysis performed for both autoclave and in-pile test samples (Fig. 5), a difference of the hydrides distributions was observed, which may be related both to test conditions and alloy compositions. Hydrides in the claddings after oxidation in the reactor are non-uniformly distributed along the cladding wall thickness, which is especially observed

in cross sections of the E110M and E635M alloys (Fig. 5b). This fact is related to a temperature gradient along the wall thickness during the irradiation test. Longest hydrides were observed in the E635M alloy cladding comparing with claddings from other alloys. The preferential orientation of hydrides for all the tests materials is tangential.

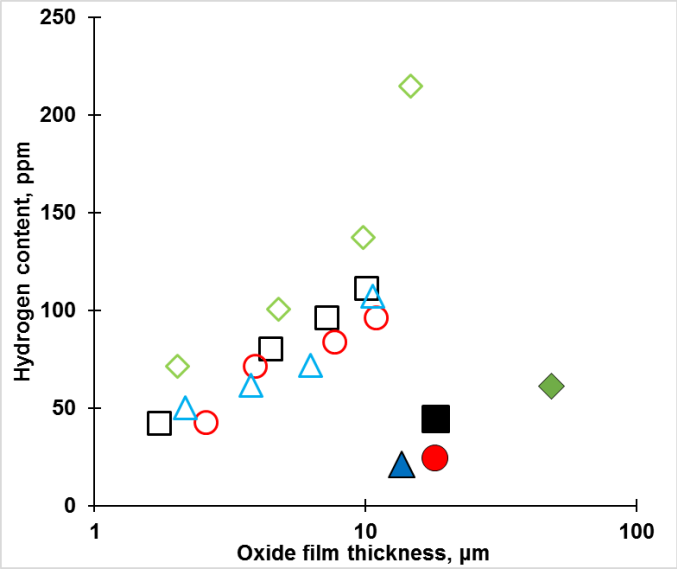

Fig.4 – Hydrogen content depending on oxide thickness in cladding samples in autoclave (empty markers) in comparison with fuel rod claddings in reactor (solid markers): E110opt (■,□),E110M (●,○), E125 (▲, △), E635M (◆,◇)

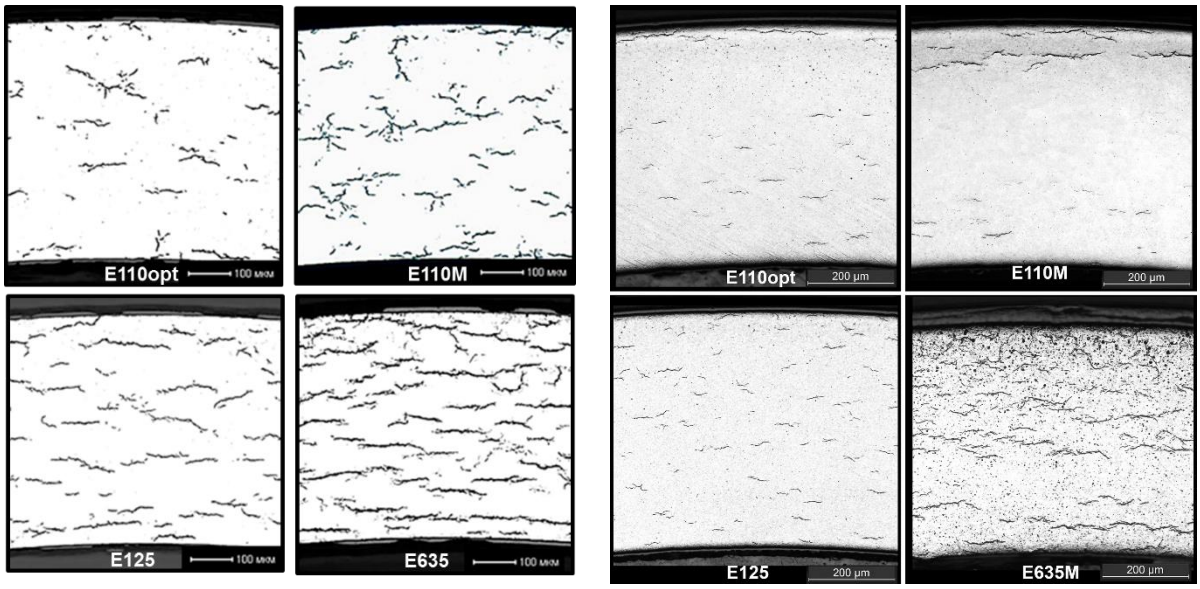

a b

Fig.5 – Hydrides distribution in claddings after autoclave (a) and in-reactor (b) tests

4. Results on creep strain resistance

To estimate the fuel cladding resistance to irradiation creep it is necessary to analyze fuel rod cladding elongation during the irradiation and data on the cladding diameter change measured after irradiation accounting for some difference in the determined fuel burnup distribution shown in Figure 1.

Averaged results determined from the fuel rods elongation measurements determined at the end of irradiation are shown in Figure 6. Minimum elongation by the end of tests was observed in the fuel rod with E635M cladding. Maximum elongation was detected in fuel rods

with E125 cladding. Fuel rod claddings from the E110opt and E110M alloys show intermediate and close to each other measured elongations with somewhat prevailing creep resistance of E110M cladding.

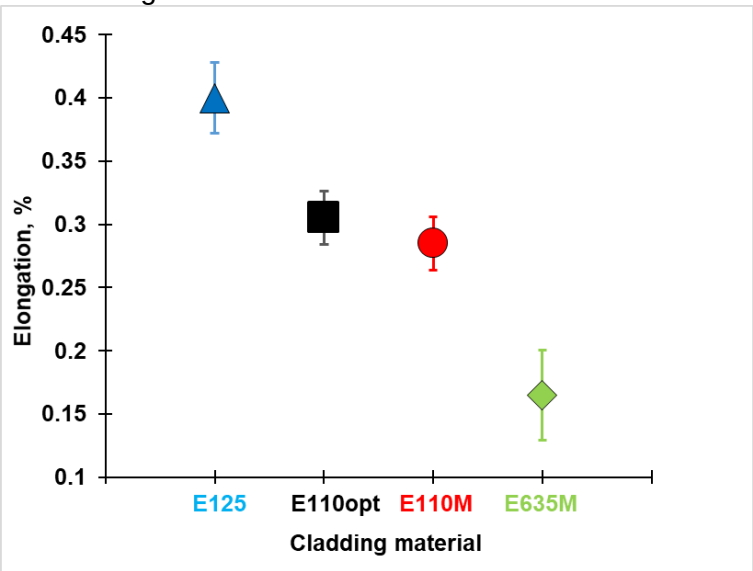

Fig. 6 – Fuel rod elongation after 907 days irradiation in Halden reactor

Diameter tracing measurements conducted along the test fuel rods with E110opt, E110M and E125 claddings alloys before and after irradiation in the Halden reactor are shown in Figure 7(a,b,c). Specific peaks observed in the diagrams of the measurements indicated that these claddings are in contact with fuel after irradiation, whereas no such peaks clearly observed in diagrams for fuel rod with claddings from E635M alloy (Figure 7d) due to lower creep of this alloy and diameter was increased because of the high oxide layer thickness (up to 60 μm).

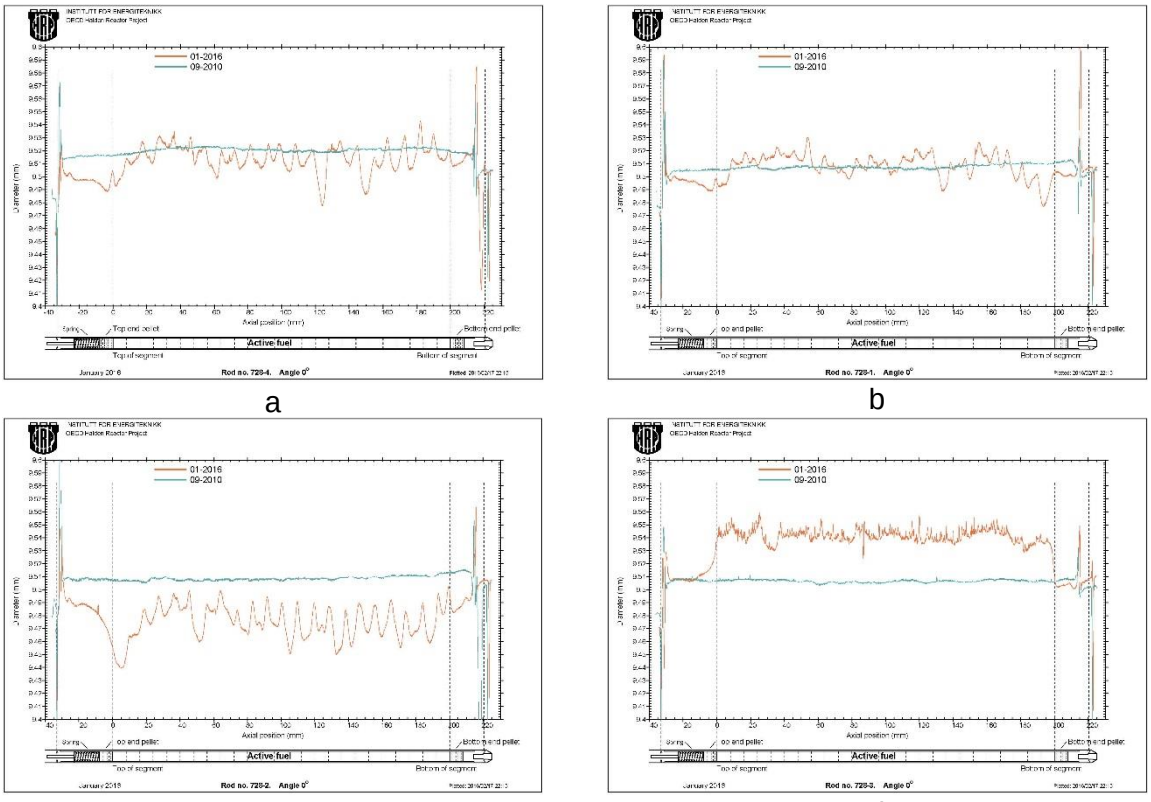

a b c d

Fig. 7 – Results of fuel rod diameter changes of alloys E110opt (a), E110M (b), E125 (c) and E635M (d) before and after irradiation

Since the data on fuel rod diameter tracings have been obtained after the entire irradiation, the gap closure time cannot be defined to compare a diametric creep rate of the alloys employed in the test.
Comparison of the diametric creep rates under irradiation of fuel rod claddings made of the alloys of interest were conducted by means of pressurizing of the cladding samples with internal pressure and irradiated in the research reactor BOR-60 which used for similar tests [11]. Clad samples for this test were taken from the same batches of claddings sent for testing in Halden reactor. Irradiation was conducted in the temperature range of 315-325 ºC under internal pressure correspondent to the 100 MPa hoop stress and at the neutron fluence of about $5.37 \cdot 10^{26}$ m^{-2} (E>0.1 MeV). Diameter measurements were done in the mid-length part of samples in two perpendicular directions before and after irradiation in the reactor. Figure 8 shows the data on the diametric creep strain of the cladding samples for the four alloys after irradiation in the BOR-60. It is seen that the E635M alloy shows minimum diametric creep strain, maximum irradiation creep rate was observed in E125 cladding sample whereas E110opt and E110M alloys showed the moderate creep strains similar to those derived from the irradiation test in the Halden reactor. However, the diametric creep strains measured after irradiation in BOR-60 in the E110M samples was significantly less than in E110opt clad samples.

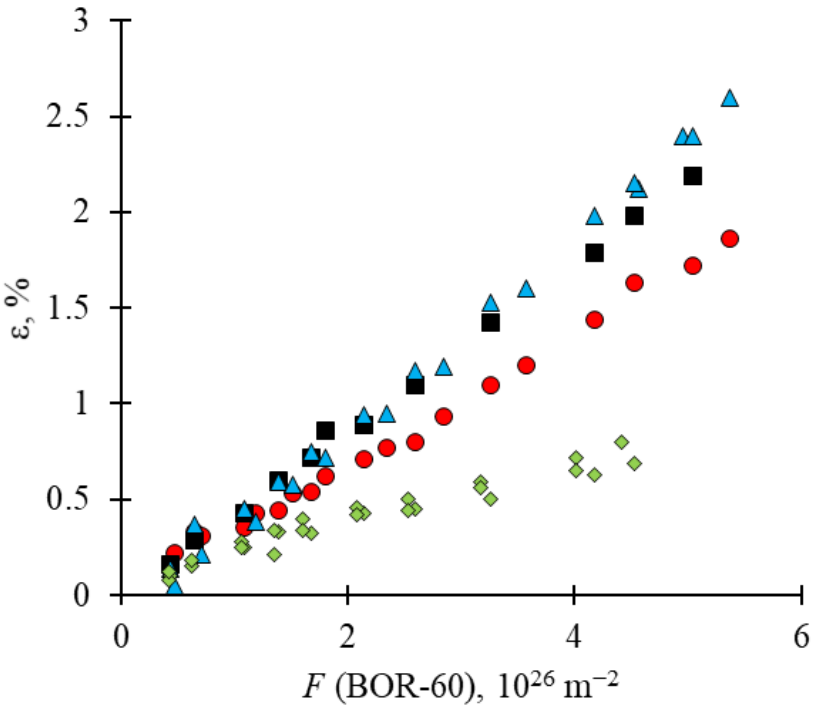

Fig. 8 – Diametric creep strain of samples under internal pressure at the 100 MPa stress of claddings from alloys E110opt (■), E110M (●), E125 (▲), E635M (◆) at the irradiation temperature 315-325 °C in the BOR-60 reactor

5. Conclusion

The results of the in-pile test carried out in the Halden reactor under advanced PWR conditions with high lithium concentration (up to 10 ppm) and PIE have shown that:
• The best corrosion and hydrogenation resistance but the worst elongation creep resistance under irradiation was observed on the fuel rod claddings made of the E125 alloy. The worst corrosion and hydrogenation resistance with the best elongation resistance under irradiation was observed on the fuel rod claddings made of the E635 alloy;
• The optimal combination of corrosion, hydrogenation and elongation resistances in reactor was observed in fuel rod claddings from the E110opt and E110M alloy. At the same time, the

E110M alloy has the better resistance to irradiation creep of the cladding comparing with the E110opt alloy with practically similar corrosion resistance.

6. References

1. Shebaldov, P. V., Peregud, M. M., Nikulina, A. V., Bibilashvili, Y. K., Lositski, A. F., Kuz'menko, N. V., Belov, V. I., and Novoselov, A. E., "E110 Alloy Cladding Tube Properties and Their Interrelation with Alloy Structure-Phase Condition and Impurity Content," Zirconium in the Nuclear Industry, ASTM STP1354, G. P. Sabol, and G. D. Moan, Eds., ASTM International, West Conshohocken, PA, 2000, pp. 545–557.
2. Shishov, V. N., Markelov, V. A., Nikulina, A. V., Novikov, V. V., Peregud, M. M., Shevyakov, A. Yu., Volkova, I. N., Kobylyansky, G. P., Novoselov, A. E., and Obukhov, A. V., "Corrosion, Dimensional Stability and Microstructure of VVER-1000 E635 Alloy FA Components at Burnups up to 72 MWday/kgU," Zirconium in the Nuclear Industry, ASTM STP1543, R. J. Comstock, and P. Barberis, Eds., ASTM International, West Conshohocken, PA, 2013, pp. 628–650.
3. Kaczorowski, D., Chabretou, V., Thomazet, J., Hoffmann, P.-B., Sell, H.-J., and Garner, G., "Corrosion Behavior of Alloy M5™: Experience Feedback," presented at Water Reactor Fuel Performance Meeting, Seoul, Korea, October 19–23, 2008—unpublished.
4. Sabol, G. P., "ZIRLO™—an Alloy Development Success," Zirconium in the Nuclear Industry, ASTM STP1467, P. Rudling, and B. Kammenzind, Eds., ASTM International, West Conshohocken, PA, 2005, pp. 3–24.
5. Takabatake, H., Abeta, S., and Murata, T., "Development Program of J-Alloy™, High Corrosion-Resistant Alloy for PWR Fuel Cladding Tube," presented at TopFuel 2006, Salamanca, Spain, October 22–26, 2006—unpublished.
6. Chabretou, V., Hoffmann, P. B., Trapp-Pritsching, S., Garner, G., Barberis, P., Rebeyrolle, V., and Vermoyal, J. J., "Ultra Low Tin Quaternary Alloys PWR Performance—Impact of Tin Content on Corrosion Resistance, Irradiation Growth, and Mechanical Properties," Zirconium in the Nuclear Industry, ASTM STP1529, M. Limback, and P. Barberis, Eds., ASTM International, West Conshohocken, PA, 2010, pp. 801–826.
7. Pan, G., Long, C. J., Garde, A. M., Atwood, A. R., Foster, J. P., Comstock, R. J., Hallstadius, L., Nuhfer, D. L., and Baranwal, R., "Advanced Material for PWR Application: AXIOM™ Cladding," presented at TopFuel 2010, Orlando, FL, September 26–29, 2010—unpublished.
8. Jeong, Y. H., Park, S.-Y., Lee, M.-H., Choi, B.-K., Bang, J.-G., Baek, J.-H., Park, J.-Y., Kim, J.-H., Kim, H. G., and Jung, Y.-H., "Development of Advanced Zr Alloys (HANA) for High Burn-Up Fuel," presented at International Meeting on LWR Fuel Performance, Kyoto, Japan, October 2–6, 2005—unpublished.
9. Nakata, M. and Hauso, E., "Summary of Characterisation Data on Cladding Materials Used in the Corrosion Test IFA-638 and in the Creep Test IFA-617," OECD Halden Reactor Project Final Report, HWR-566, 1998.
10. Bennett, P., Stoenescu, R., and Karlsen, T., "The PWR Corrosion and Hydriding Test IFA-638," OECD Halden Reactor Project Final Report, HWR-840, 2010.
11.Shishov V.N., Peregud M.M., Nikulina A.V., Kon'kov V.F., Novikov V.V., Markelov V.A., Khokhunova T.N., Kobylyansky G.P., Novoselov A.E., Ostrovsky Z.E., Obukhov A.V. Structure-Phase State, Corrosion and Irradiation Properties of Zr-Nb-Fe-Sn System Alloys // Zirconium in the Nuclear Industry: 15th Int. Symp. ASTM STP 1505. 2009. P. 724-743 (Journal of ASTM International. Vol. 5. No. 3. Paper ID JAI101127).